IS06/10:
Petrographic, petrophysical and geochemical characterisation of the northern Porcupine High using recently recovered MeBo shallow cores

Interim report, June 2007

J.S. Daly, S. Tyrrell, P.D.W. Haughton and P.M. Shannon.
UCD School of Geological Sciences, University College Dublin
E-mail: shane.tyrrell@ucd.ie

Background:
A program of sea floor drilling (MeBo) was carried out by the Petroleum Affairs Division (PAD) on the northern Porcupine Bank during July 2006. Core was recovered from two sites within Quadrant 25 – site BII and site L, corresponding to cores 25/7-sb(MeBo)3 and 25/27-sb(MeBo)2 respectively. A total thickness of 1.35 m was penetrated in 25/7–sb(MeBo)3, from which 0.8m core of *in-situ* orthogneiss (the main topic of this report) was recovered at base. The 25/27-sb(MeBo)2 borehole penetrated 8.58m, and the recovered core has been provisionally interpreted as a weakly-cemented calcareous matrix-supported breccia/conglomerate, comprising pebbles and blocks of a variety of metamorphic rock-types (amphibolites and gneiss).

The importance of the Porcupine High as a potential source for Jurassic sandstones in the North Porcupine Basin has been highlighted by the recent pilot provenance study (IS05/19), which indicates that it may also be an important structural feature during the Cretaceous. However, the nature of the Porcupine High, its age, crustal affinity, and its uplift history has never been determined through direct sampling. These cores, therefore, offer a unique opportunity to characterise this important portion of the Irish Continental Shelf. Understanding the nature of the source area of a reservoir sandstone provides important constraints on the mineralogy and, therefore, on the reservoir characteristics of the sandstones.

Work to date:
The work carried out to date has focussed on characterising and classifying the 0.8m core of *in-situ* rock recovered from site BII, core 25/7-sb(MeBo)3 (Fig. 1). These studies have involved optical microscopy, scanning electron microscopy (SEM), cathodoluminescence (CL) and electron microprobe analysis (EMPA). This approach has enabled the petrography of the rock to be described and has allowed the chemical composition of the feldspar and the garnet to be determined. The BSE/CL feldspar images obtained will be used to guide Pb analysis using LA-MC-ICPMS.

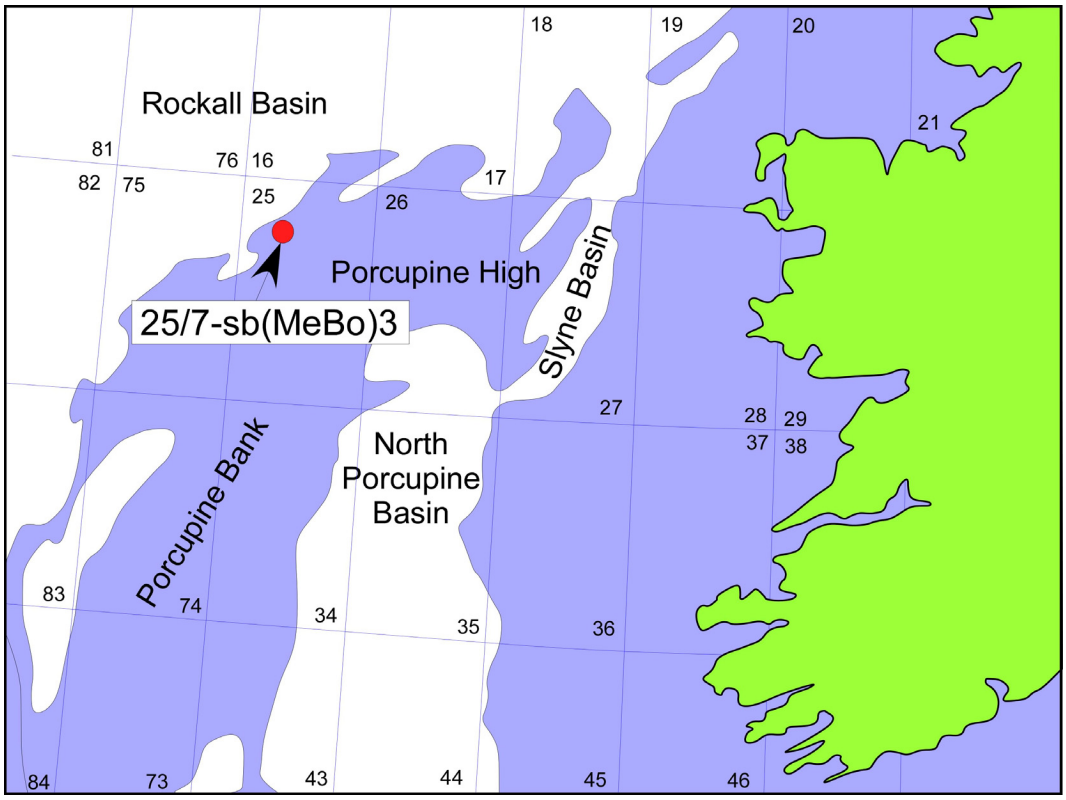

Figure 1: Map showing the location of site BII on the Porcupine High, from which core 25/7-sb(MeBo)3 was recovered.

Results to date:

Hand specimen description

Material cored at site BII, (core 25/7-sb(MeBo)3) comprises a single lithology hitherto described as "granite" (pers. comm. N. Murphy, PAD). The rock comprises randomly orientated pink K-feldspar megacrysts up to 2.5 cm set in a darker matrix of quartz, feldspars and ferromagnesian minerals (Fig. 2). The K-feldspar megacrysts are surrounded by c. 2-4 mm rims of pale grey plagioclase feldspar (Fig. 3). High grade metamorphism is manifest by the presence of ringlets of fine-grained (up to1 mm-diameter) garnet crystals surrounding the megacryst rims and by an overall polygonal granular texture typical of granulite-facies metamorphism.

Optical microscopy

Two thin sections, one of which has been polished for electron microprobe analysis and scanning electron microscopy, were made from a small fragment of broken core.

The K-feldspar megacrysts, which probably represent relict igneous phenocrysts, are extensively recrystallized to a granular aggregate of polygonal K-feldspar and occasional plagioclase grains, both typically 2-3 mm across (Fig. 4a). Within the outer 4 mm of the megacrysts, K-feldspar gives way to c. 2.5 mm grains of plagioclase (Fig. 4b, probably representing original "rapakivi" rims), which are in turn surrounded by irregular ringlets of polygonal garnet, up to 0.8 mm across. This texture is possibly the result of garnet growth (and consumption of plagioclase) in response to increasing pressure due to tectonic loading.

Figure 2: Photograph of K-feldspar megacrystic granulitic orthogneiss from the Porcupine High (25/7-sb (MeBo)3) showing randomly orientated K-feldspar megacrysts (pink) displaying rapakivi texture (grey rims) set in a darker matrix comprising quartz, feldspar and mafic minerals. Photograph courtesy of Mr N. Murphy, Petroleum Affairs Division.

The matrix comprises irregularly alternating domains (bands) of predominantly mafic or felsic minerals, usually several cm long and up to 1 cm wide in which the mafic minerals are sometimes aggregated in equant clots from 6mm to 1 cm across. The mafic minerals comprise garnet, clinopyroxene, biotite, opaques and hornblende. Within the mafic bands, grain aggregates and individual grains of biotite have a preferred orientation parallel to the banding, resembling a foliation (Fig. 4c). However, the foliation does not appear to persist through the rock and is apparently developed locally parallel to the K-feldspar megacryst faces. The mafic minerals are generally in textural equilibrium (Fig. 4d) with the exception of hornblende, which forms porphyroblasts up to 2 mm across (Fig. 4e) with inclusions of quartz, opaques, zircon and apatite and is probably a late retrogressive phase replacing clinopyroxene (Fig. 4d).

Zircon (up to at least 300 mm long) and apatite (typically 200 mm across) are present (Fig. 4f) in both mafic and felsic domains, likely sufficient in abundance for U-Pb and fission track dating respectively.

Scanning Electron Microscopy

K-feldspar

Backscattered electron microscopy (BSE) images of the K-feldspar megacrysts reveal fine- to medium-scale perthitic exsolution (lamellae ranging from 1 – 20 μm thick), albitic veins and inclusions mainly of albite and quartz (Fig. 5a-e). Cathodoluminescence (CL) images captured from the same megacrysts are less revealing, but there are subtle variations in the strength of the signal (light-dark areas, see figures 5a-e), which may, in some way, reflect original compositional zoning, or,possibly, variations in the levels of intra-grain alteration.

Garnet

Four garnet crystals were imaged using BSE (Fig. 6). These images show fractured garnet crystals with abundant rounded inclusions of quartz, but little variation in signal strength across single crystals.

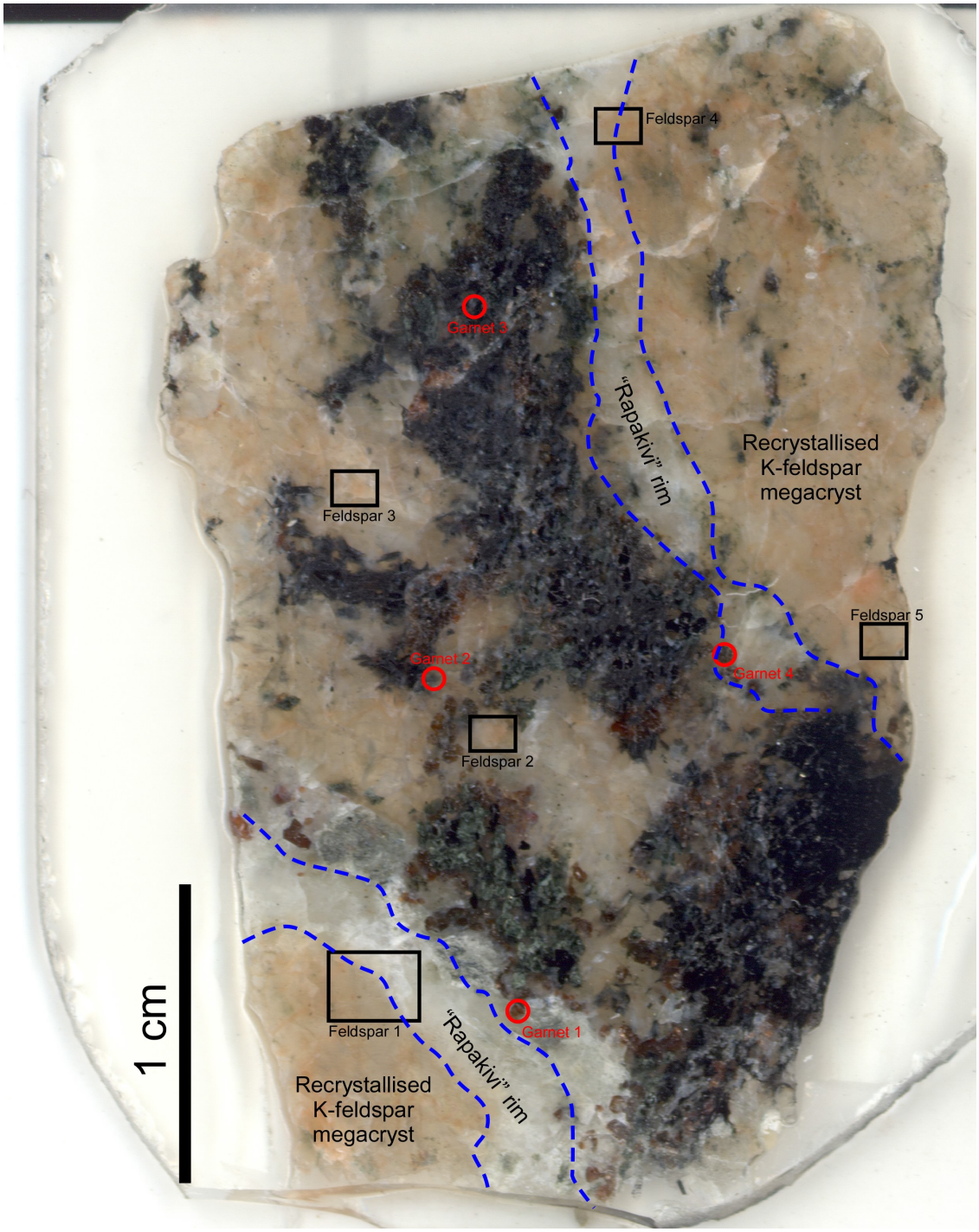

Figure 3: Scanned polished section showing recrystallised K-feldspar megacrysts with "Rapakivi" rims and the position of BSE/CL images (Fig. 5, 6)

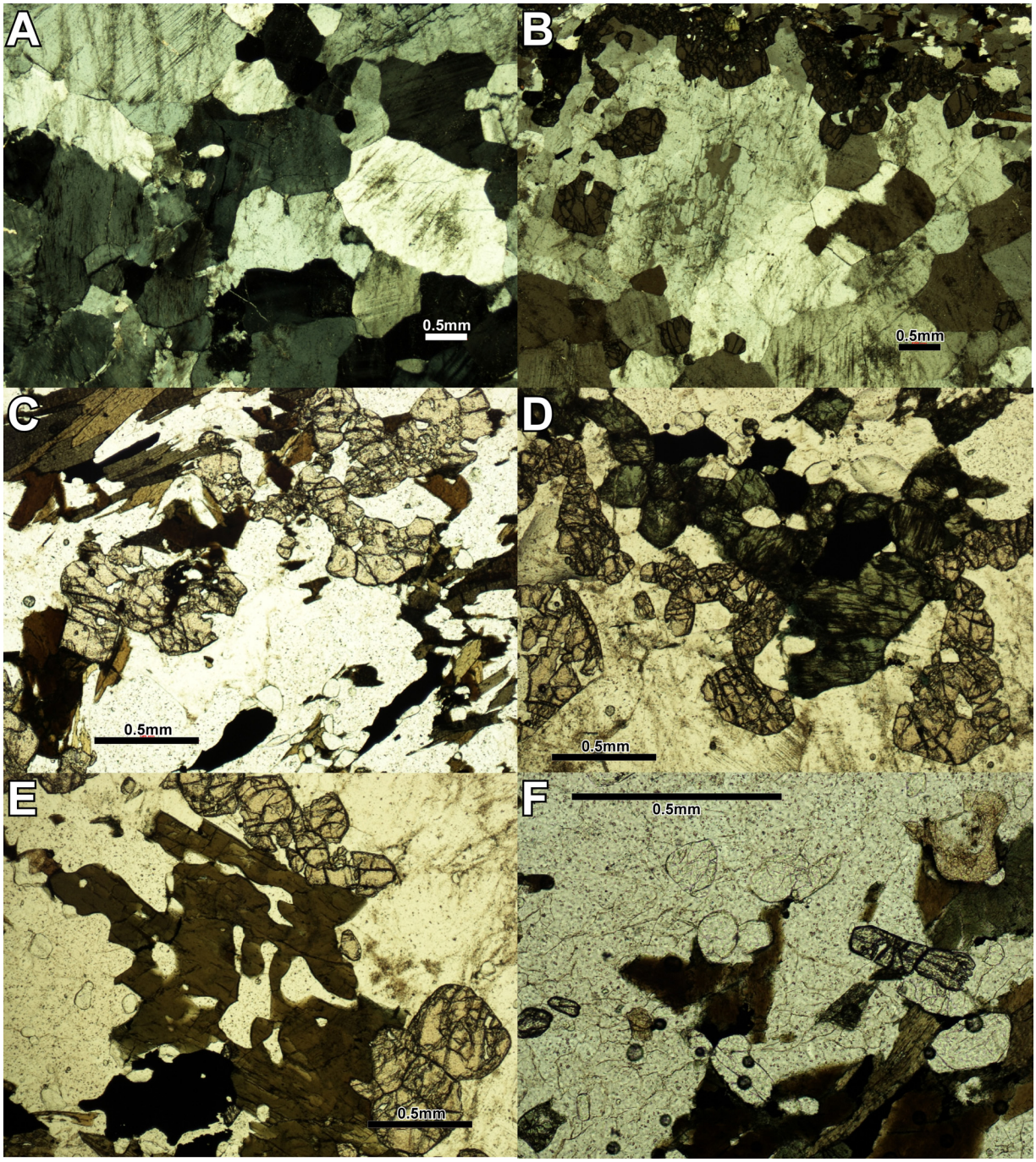

Figure 4: Photomicrographs of thin section of the orthogneiss. A) Interior of a recrystallised K-feldspar megacryst comprising a polygonal granular aggregate of K-feldspar and occasional plagioclase grains.B) Rim of a recrystallised K-feldspar megacryst comprising a polygonal granular aggregate plagioclase grains, surrounded by ringlets of garnet. This texture is consistent with garnet growth in response to increasing pressure (e.g. tectonic loading). C) Aligned aggregates of garnet and biotite in a mafic domain resembling a foliation. It is unclear if the alignment is a true foliation or a local feature parallel to the surface of the adjacent K-feldspar megacryst.D)Polygonal aggregate of clinopyroxene together with opaques, plagioclase, garnet and apatite, all in textural equilibrium (apart from incipient replacement of the clinopyroxene by hornblende).E) Texturally late hornblende porphyroblast, with prominent in inclusions of quartz, advancing on garnet and an opaque (Fe-Ti oxide). F) Accessory zircon and apatite, which probably represent original magmatic phases, near the contact between a mafic and felsic band.

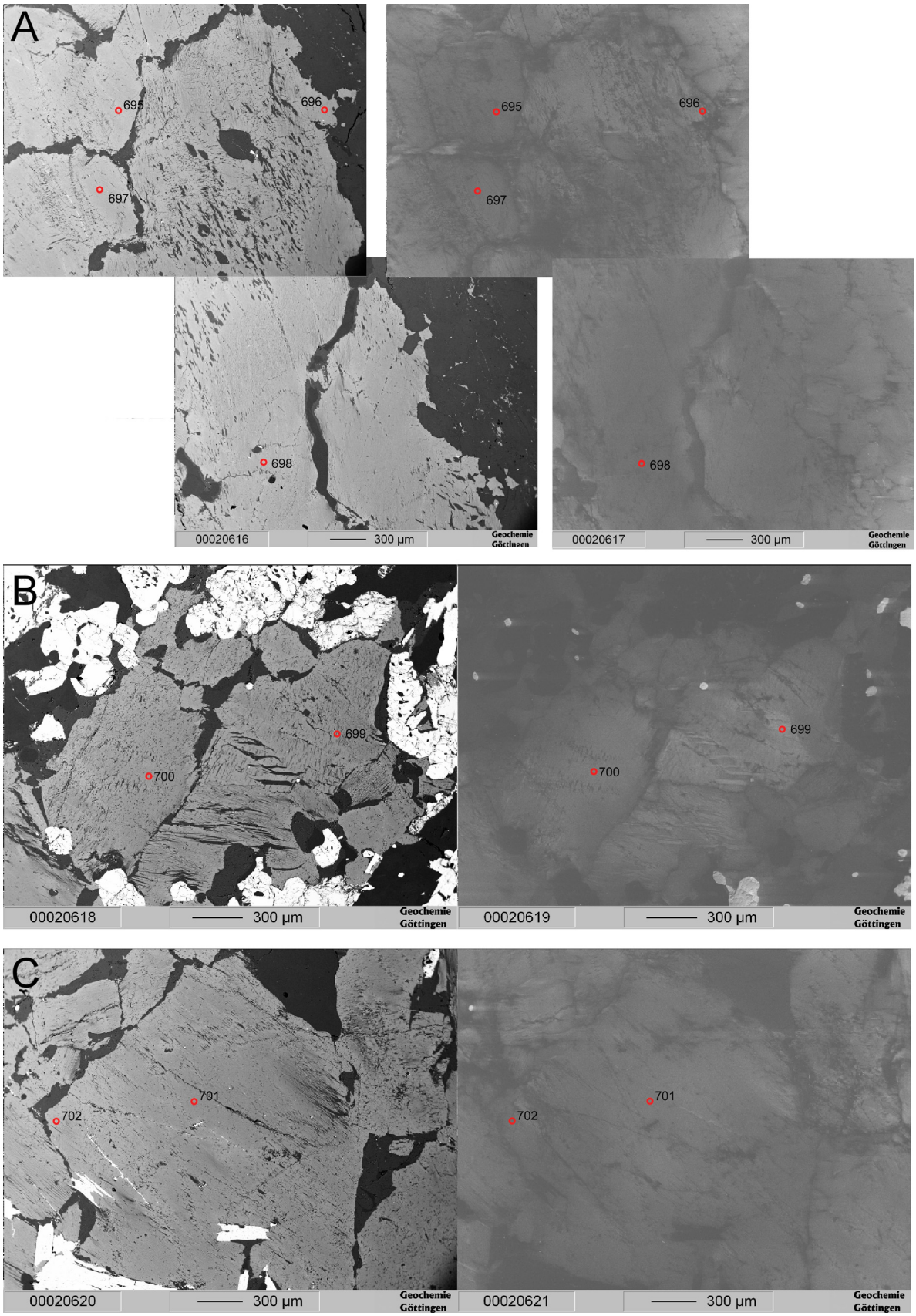

Figure 5 (*continued overleaf*): Backscattered electron microscope (BSE, left) and cathodoluminescence (CL, right) images of parts of 5 recrystallised K-feldspar megacrysts (Feldspars 1-5; Fig. 3, corresponding with images A-E above) showing the position of electron microprobe analysis spots.

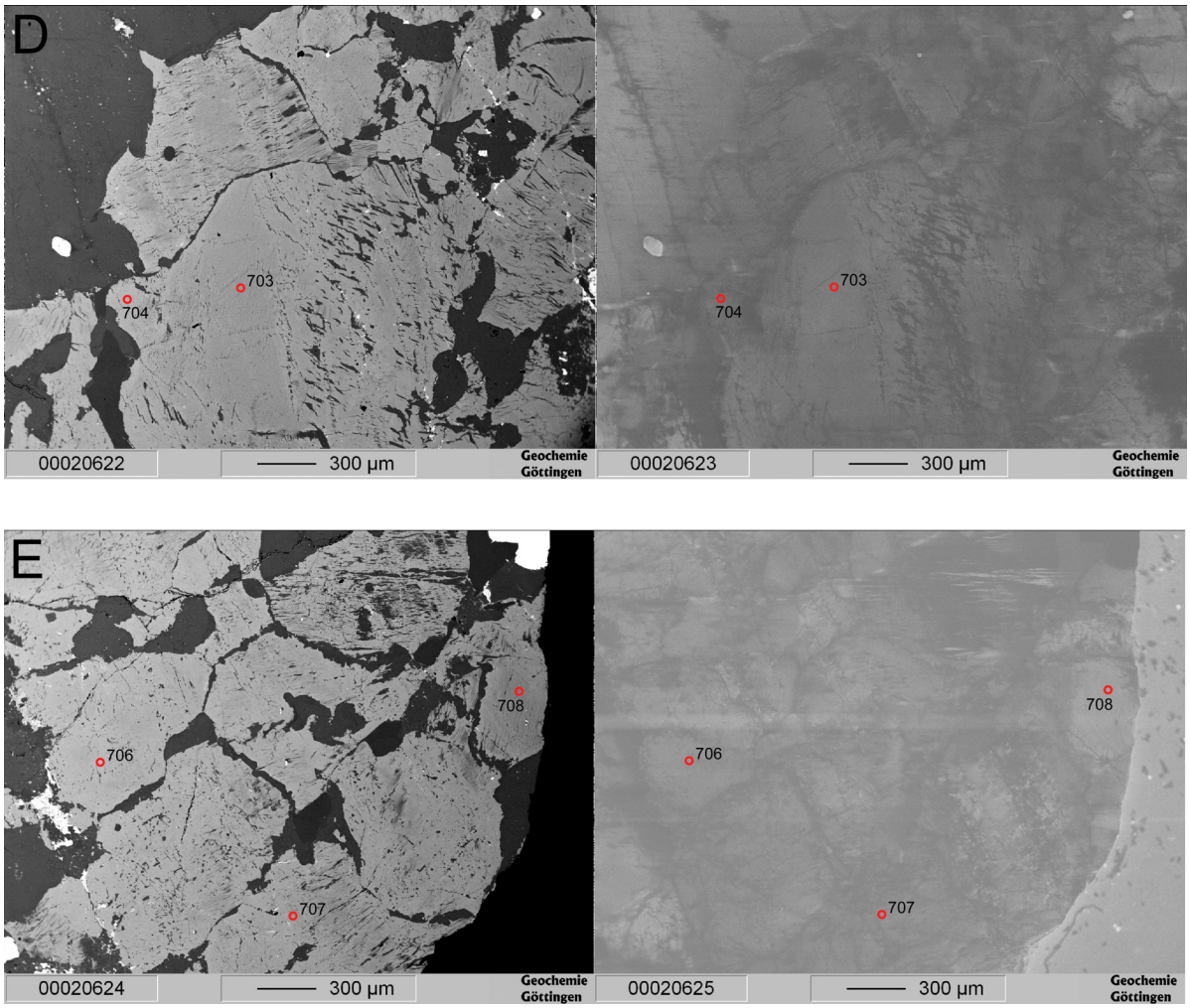

Figure 5 (*continued*): Backscattered electron microscope (BSE, left) and cathodoluminescence (CL, right) images of parts of 5 recrystallised K-feldspar megacrysts (Feldspars 1-5; Fig. 3, corresponding with images A-E above) showing the position of electron microprobe analysis spots.

Mineral Chemistry

K-feldspar

Electron microprobe analytical spots (Fig. 5) were targeted within the K-feldspar megacrysts in order to determine the major element composition and to detect any intracrystalline chemical zoning both in major elements and in Fe, Ba and Sr. The electron microprobe data (Table 1) constrain the composition of the crystal at the specific spot, though not the bulk composition of the megacryst. Major element data indicate that the composition of the K-feldspar varies from $Or_{95}Ab_5$ to $Or_{75}Ab_{25}$ (Fig. 7). Ab content varies within individual crystals, but there is no consistent variation relative to the position of the analysed spot within the crystal. There is no clear link between CL signal strength and trace element composition, indicating that the CL signal may be a related of the concentration of an unanalysed trace component.

Garnet

Electron microprobe analysis profiles were measured across four garnet crystals in order to constrain the bulk composition and to investigate any compositional variations. The garnets

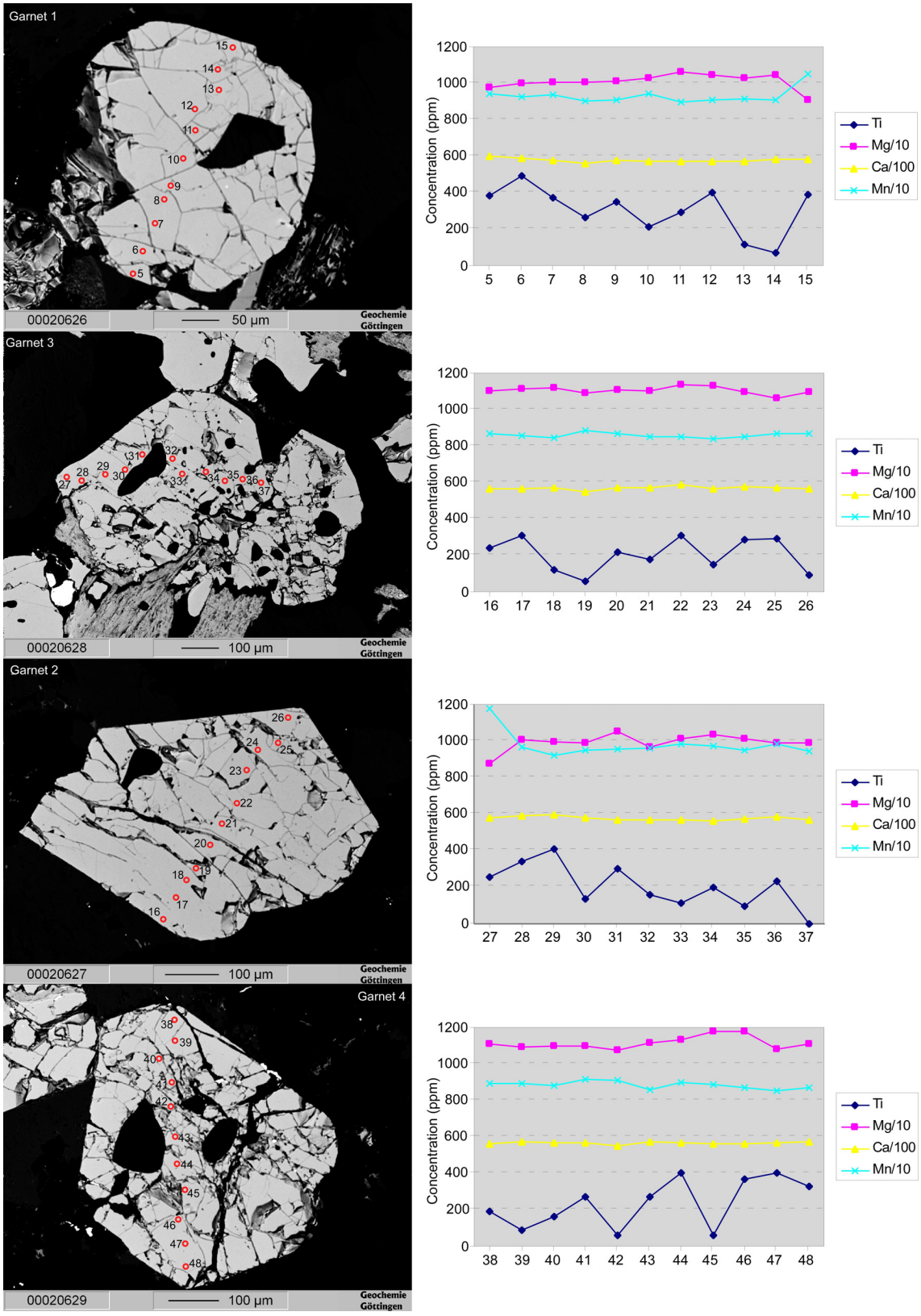

Figure 6: BSE images of garnet crystals 1-4 showing the position of electron microprobe analysis points and line profiles of trace elements (Ca, Mg, Mn, Ti).

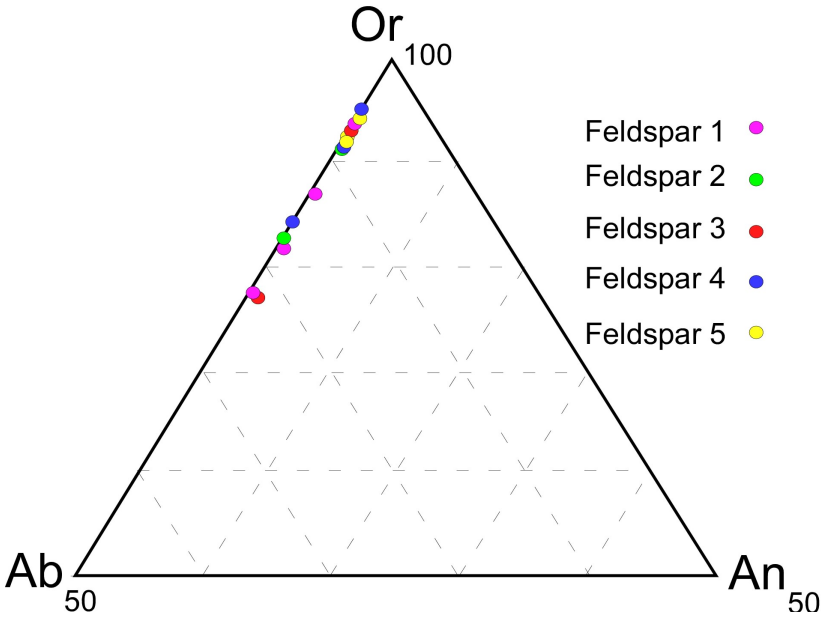

Figure 7: Ternary plot (Orthoclase; Or, Albite; Ab, and Anorthite; An) illustrating the composition of the analysed spots within the recrystallised K-feldspar megacrysts.

($Alm_{68}Grs_{22}Prp_{7}Sps_{3}$) are predominantly almandine (Fe) with minor grossular (Ca) and lesser amounts of pyrope (Mg) and spessartine (Mn). Only minor chemical zoning is present (Figs. 6, 8), consistent with high temperature granulite-facies metamorphism. Either growth zoning was absent or it has been lost through intracrystalline diffusion. Any chemical zoning that is present is difficult to interpret in the absence of chemical data from other ferromagnesian phases. However several garnets display strong increases in Fe/Mg towards the rims (Fig. 8) suggesting retrograde zoning due to exchange of Fe and Mg between garnet and other minerals (e.g. clinopyroxene, biotite and hornblende). This suggests that the rock experienced slow cooling after metamorphism. Further data (principally EMPA analyses of plagioclase, clinopyroxene and biotite) are required to explore this possibility and to allow calculation of equilibrium metamorphic pressure and temperature values.

Work in progress:
Selection of sub-samples for petrophysical measurements and mineral separation is under way. Large zircon crystals are evident in thin section (Fig. 4d) showing that mineral separation is likely to yield sufficient of this mineral for U-Pb geochronology.

Further electron microprobe analyses will be carried out in July 2007 on a polished thin section, awaiting analysis at the University of Göttingen. This will enable the calculation of metamorphic PT conditions.

Work planned:
Mineral separation will be undertaken shortly with a view to recovering zircon for U-Pb geochronology and apatite for fission track analysis. Give the high abundance of these trace minerals, it is planned to carry out mineral separation using small fragments that have broken from the core thereby preserving larger pieces for petrophysical and whole-rock geochemical analyses. U-Pb geochronology will be carried out at the NORDSIM ion microprobe laboratory at the Swedish Museum of Natural History, Stockholm. Pb isotopic analysis of the K-feldspar by LA-MC-ICPMS

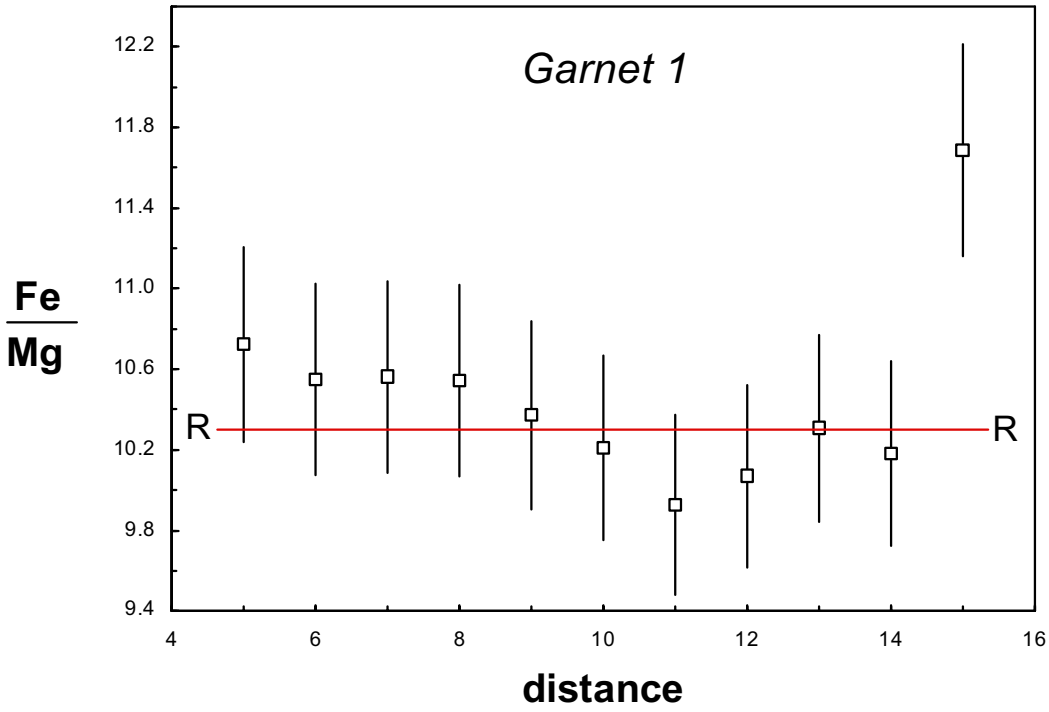

Figure 8: Plot of Fe/Mg ratio with estimated error bars along a rim to rim profile within Garnet 1 crystal (Fig. 6) illustrating a lack of zoning (indistinguishable within analytical error) except at one rim (R) where the Fe/Mg ratio increases significantly, possibly due to retrograde exchange with another ferromagnesian phase as a result of slow cooling following high temperature metamorphism.

will be undertaken on the same thin section used for EMPA analysis and already imaged by SEM (see below).

Determination of the petrophysical properties, including density and seismic velocity, will be carried out with Professor Matt Salisbury, Natural Resources Canada, Dartmouth, Nova Scotia.

Samples for apatite fission track analysis, to be carried out in collaboration with Dr David Chew, Trinity College Dublin, will be sent for irradiation as soon as possible.

XRF analysis of a representative whole-rock sample, will be carried out at the University of Leicester, while Sm-Nd and Rb-Sr whole-rock isotopic analyses will be carried out by isotope dilution thermal ionisation mass spectrometry (IDTIMS) at UCD.

Amendment to original work plan:
For logistic reasons beyond our control it will not be possible to complete the work plan until the end of 2007. It will not be possible to obtain U-Pb analyses by ion microprobe until the autumn because there are no bookings available at the NORDSIM ion microprobe lab. until then.

A major goal of the project is to characterize the Porcupine High sample in terms of its Pb isotopic composition as a possible source of detrital K-feldspar. Unfortunately the Copenhagen laboratory, hitherto the only facility where the appropriate method has been set up, is not available. It is hoped instead that the Pb analysis can be undertaken at Memorial University, Newfoundland. Dr Tyrrell will visit Memorial in July, under the auspices of NAPSA, to discuss how this can be done in cooperation with Professor P. Sylvester.

Arrangements have been made to carry our petrophysical measurements (density and sonic velocity) with Dr Matt Salisbury. However high precision drilling of suitable mini-cores must first be undertaken, probably at University College London, for which a booking is as yet not confirmed. Once the drilling has been completed, the drilled out core segment will be crushed for whole-rock major and trace element and isotopic analysis.

Table 1: Electron Microprobe point data from K-feldspar crystals in Porcupine High sample PH1

Feldspar 1	695	696	697	698	Average
SiO2 (wt%)	65.08	64.31	60.46	65.59	63.86
Na2O (wt%)	1.99	0.5998	1.42	2.51	1.63
K2O (wt%)	13.87	16.14	14.6	13.11	14.43
CaO (wt%)	0.0846	0.066	0.08	0.0824	0.0783
SrO (wt%)	0.0609	0	0.0327	0.0609	0.0386
Al2O3 (wt%)	18.76	18.4	18.42	18.98	18.64
BaO (wt%)	0.5592	0.526	0.5682	0.6357	0.5723
FeO (wt%)	0.0158	0.0116	0.0454	0.0329	0.0264
Wt-total	100.42	100.05	95.62	100.99	99.27

Feldspar 2	699	700	Average
SiO2 (wt%)	65.35	64.48	64.92
Na2O (wt%)	0.9397	1.94	1.44
K2O (wt%)	15.28	13.84	14.56
CaO (wt%)	0.0789	0.0512	0.0651
SrO (wt%)	0	0.0334	0.0167
Al2O3 (wt%)	18.78	18.85	18.82
BaO (wt%)	0.4712	0.4582	0.4647
FeO (wt%)	0.0194	0.0244	0.0219
Wt-total	100.91	99.68	100.30

Feldspar 3	701	702	Average
SiO2 (wt%)	61.96	65.44	63.70
Na2O (wt%)	2.32	0.6282	1.47
K2O (wt%)	12.31	15.95	14.13
CaO (wt%)	0.188	0.0275	0.1078
SrO (wt%)	0.0228	0.0468	0.0348
Al2O3 (wt%)	21.78	18.54	20.16
BaO (wt%)	0.4405	0.4031	0.4218
FeO (wt%)	0.0655	0.0513	0.0584
Wt-total	99.09	101.08	100.09

Feldspar 4	703	704	705	Average
SiO2 (wt%)	65.51	65.09	64.99	65.20
Na2O (wt%)	1.76	0.5599	0.8307	1.05
K2O (wt%)	14.29	16.05	15.67	15.34
CaO (wt%)	0.0339	0.0198	0.0373	0.0303
SrO (wt%)	0.045	0.024	0.007	0.0253
Al2O3 (wt%)	18.69	18.52	18.83	18.68
BaO (wt%)	0.4816	0.4385	0.5606	0.4936
FeO (wt%)	0.0269	0.0304	0.0213	0.0262
Wt-total	100.84	100.73	100.95	100.84

Feldspar 5	706	707	708	Average
SiO2 (wt%)	65.52	64.89	65.33	65.25
Na2O (wt%)	0.6886	0.5779	0.7947	0.6871
K2O (wt%)	15.82	16.03	15.7	15.85
CaO (wt%)	0.0466	0.0262	0.0386	0.0371
SrO (wt%)	0.0378	0.0339	0.066	0.0459
Al2O3 (wt%)	18.62	18.55	18.38	18.52
BaO (wt%)	0.4919	0.6031	0.4367	0.5106
FeO (wt%)	0	0.0454	0.0371	0.0275
Wt-total	101.22	100.76	100.78	100.92

Table 2: Electron microprobe data from profiles along four garnet crystals from sample PH1 (see Figure ?)

Garnet 1	5	6	7	8	9	10	11	12	13	14	15	Average
SiO2 wt%	38.01	37.90	38.02	38.13	37.80	37.94	37.88	37.80	37.97	38.00	37.81	37.93
Na2O wt%	0.0312	0.0218	0.0000	0.0199	0.0000	0.0000	0.0000	0.0129	0.0104	0.0000	0.0000	0.0087
K2O wt%	0.0086	0.0156	0.0064	0.0209	0.0000	0.0100	0.0000	0.0000	0.0137	0.0000	0.0000	0.0068
TiO2 wt%	0.0637	0.0818	0.0620	0.0436	0.0586	0.0353	0.0490	0.0663	0.0195	0.0111	0.0647	0.0505
FeO wt%	31.05	31.17	31.45	31.39	31.07	31.13	31.15	31.06	31.43	31.40	31.47	31.25
Al2O3 wt%	20.81	20.76	20.88	20.83	20.97	20.80	20.84	20.89	20.83	20.75	20.57	20.81
MgO wt%	1.62	1.66	1.67	1.67	1.68	1.71	1.76	1.73	1.71	1.73	1.51	1.68
CaO wt%	8.37	8.21	8.11	7.87	8.04	7.99	7.99	8.00	8.00	8.16	8.18	8.08
MnO wt%	1.22	1.19	1.21	1.17	1.18	1.22	1.15	1.17	1.18	1.17	1.36	1.20
wt-total	101.19	101.01	101.41	101.14	100.80	100.82	100.82	100.74	101.18	101.23	100.97	101.03

Garnet 2	16	17	18	19	20	21	22	23	24	25	26	Average
SiO2 wt%	37.91	37.93	37.71	37.74	38.01	38.07	38.09	37.81	37.97	38.11	37.93	37.93
Na2O wt%	0.0297	0.0099	0.0000	0.0000	0.0000	0.0000	0.0168	0.0331	0.0104	0.0233	0.0441	0.0152
K2O wt%	0.0000	0.0000	0.0000	0.0000	0.0064	0.0000	0.0000	0.0181	0.0000	0.0075	0.0000	0.0029
TiO2 wt%	0.0405	0.0521	0.0212	0.0109	0.0370	0.0302	0.0518	0.0256	0.0480	0.0494	0.0161	0.0348
FeO wt%	30.82	30.70	30.61	31.26	31.10	30.84	30.60	30.43	30.71	30.81	30.96	30.80
Al2O3 wt%	21.03	21.15	21.16	20.78	21.07	21.17	21.36	21.28	21.05	21.05	20.94	21.09
MgO wt%	1.83	1.85	1.86	1.81	1.84	1.83	1.89	1.88	1.82	1.76	1.82	1.84
CaO wt%	7.97	7.99	8.02	7.72	8.00	8.00	8.25	7.98	8.12	8.02	7.98	8.00
MnO wt%	1.12	1.11	1.09	1.15	1.12	1.10	1.10	1.09	1.10	1.13	1.12	1.11
wt-total	100.76	100.79	100.48	100.46	101.18	101.04	101.37	100.54	100.82	100.96	100.81	100.84

Garnet 3	27	28	29	30	31	32	33	34	35	36	37	Average
SiO2 wt%	37.56	38.10	37.61	37.85	37.22	37.52	37.73	37.58	37.87	37.75	37.50	37.66
Na2O wt%	0.0000	0.0000	0.0179	0.0000	0.0259	0.0259	0.0219	0.0224	0.0413	0.0000	0.0184	0.0158
K2O wt%	0.0148	0.0121	0.0000	0.0000	0.0068	0.0090	0.0000	0.0000	0.0000	0.0201	0.0000	0.0057
TiO2 wt%	0.0424	0.0571	0.0680	0.0224	0.0507	0.0264	0.0186	0.0330	0.0161	0.0393	0.0000	0.0340
FeO wt%	31.07	31.02	31.12	30.99	31.40	31.36	31.12	31.16	31.16	31.15	31.43	31.18
Al2O3 wt%	20.50	20.46	20.48	20.43	20.54	20.56	20.75	21.15	20.86	20.48	20.70	20.63
MgO wt%	1.45	1.67	1.65	1.64	1.74	1.60	1.68	1.72	1.68	1.64	1.64	1.65
CaO wt%	8.15	8.26	8.35	8.13	7.97	7.94	7.98	7.85	8.05	8.18	7.95	8.07
MnO wt%	1.52	1.25	1.19	1.23	1.23	1.24	1.27	1.25	1.22	1.27	1.22	1.26
wt-total	100.30	100.84	100.48	100.30	100.18	100.29	100.57	100.78	100.89	100.53	100.46	100.51

Garnet 4	38	39	40	41	42	43	44	45	46	47	48	Average
SiO2 wt%	37.75	37.83	37.71	37.75	37.73	37.80	38.07	38.00	37.67	38.02	37.60	37.81
Na2O wt%	0.0000	0.0104	0.0000	0.0100	0.0388	0.0223	0.0000	0.0099	0.0000	0.0000	0.0000	0.0083
K2O wt%	0.0172	0.0000	0.0000	0.0110	0.0000	0.0000	0.0104	0.0000	0.0000	0.0000	0.0064	0.0041
TiO2 wt%	0.0324	0.0155	0.0279	0.0454	0.0103	0.0460	0.0678	0.0100	0.0615	0.0675	0.0551	0.0399
FeO wt%	31.12	30.92	30.57	30.72	31.23	30.58	30.69	31.00	31.22	31.16	31.25	30.95
Al2O3 wt%	20.63	21.23	21.17	21.05	20.91	21.14	21.26	21.10	21.29	20.83	20.64	21.02
MgO wt%	1.84	1.81	1.82	1.82	1.78	1.85	1.88	1.95	1.95	1.79	1.84	1.85
CaO wt%	7.91	8.02	7.95	7.99	7.73	8.04	7.97	7.91	7.87	7.97	8.07	7.95
MnO wt%	1.16	1.15	1.14	1.18	1.18	1.11	1.16	1.14	1.12	1.10	1.12	1.14
wt-total	100.46	101.00	100.39	100.57	100.62	100.58	101.10	101.11	101.19	100.93	100.59	100.78